Geophys. J. Int. (2001) **145,** 647–660

Gas hydrate stability and the assessment of heat flow through continental margins

Ingo Grevemeyer and Heinrich Villinger

FB Geowissenschaften, Universität Bremen, Klagenfurter Strasse, 28359 *Bremen, Germany. E-mail: ingo@geophys2.uni-bremen.de*

Accepted 2000 December 12. Received 2000 November 30; in original form 2000 July 14

SUMMARY

A prominent feature across some continental margins is a bottom-simulating reflector (BSR). This seismic reflection generally coincides with the depth predicted for the base of the gas hydrate stability field. Because the occurrence of gas hydrates is controlled by temperature and pressure conditions, it has been suggested that BSRs mark an isotherm and they have therefore been used to estimate the heat flow through continental margins; crucial parameters are the temperature at BSR depth and at the seafloor and the thermal conductivity structure between the BSR and the seabed. However, very often the required parameters are not available and therefore they have been derived from models for gas hydrate stability and empirical relationships to obtain thermal conductivities from seismic velocities. Here, we use downhole temperature, thermal conductivity, porosity and logging data from 10 Ocean Drilling Program (ODP) sites drilled into and through the gas hydrate field to investigate the quality of estimates. Our analyses and application of constraints to the Makran margin off Pakistan indicate the following. (i) The temperature at BSR depth could be approximated by a seawater–methane system, although capillary forces, chemical impurities or non-equilibrium conditions can lower (or increase) the temperature. If calibration by heat probe measurements is possible, errors of geothermal gradients are less than 10 per cent, otherwise uncertainties of 20 per cent (or even higher) may arise. In addition, seasonal variations of bottom water temperature have to be considered, because they may affect thermal gradients by up to $\sim$10 per cent. (ii) The impact of typical quantities of low-thermal-conductivity gas hydrate on the bulk thermal conductivity is insignificant. (iii) The thermal conductivity profile between the BSR and the seabed can generally be approximated by a mean value. Thus, (iv) seabed measurements should be used instead of empirical relationships, which may produce errors of 5–30 per cent. Consequently, in addition to high-quality seismic data, a prerequisite should be a large data set of thermal conductivities and oceanographic data. Heat probe measurements are recommended to constrain geothermal gradients. In this case the uncertainty of heat flow is 5–10 per cent of the estimated heat flow. If these data are not available errors/uncertainties can reach 50–60 per cent of the calculated value.

Key words: continental margins, gas hydrate, heat flow, thermal conductivity.

INTRODUCTION

Thermal properties are key factors in governing the dynamics of continental margins; for example, the updip and downdip limits of rupture during great subduction thrust earthquakes are suggested to be controlled by the thermal structure of the downgoing slab (Hyndman & Wang 1993, 1995; Oleskevich *et al*. 1999). Thermal control of the rupture extent on subduction thrusts is especially important for estimating the hazard from great earthquakes where there have been no historical events. The downdip limit determines the landward extent of the seismogenic zone; the seaward updip limit is important for the generation of large tsunami earthquakes (Pelayo & Wiens 1992). However, local variations in the heat flow are likely to reflect focused fluid flow along faults or other structurally controlled pathways (Fisher & Hounslow 1990; Davis *et al*. 1990; Zwart *et al*. 1996), which play an integral role in determining the spatial and temporal distributions of deformation at continental margins. At passive margins and sedimentary basins, heat flow and thermal history have important implications for

the maturation of basins with respect to oil and gas. Therefore, heat flow surveys serve critical purposes in oil exploration and production.

The assessment of the thermal structure of margins is generally derived from heat flow studies carried out on the seafloor. The Earth's heat loss, q, however, is not measured directly, but calculated from the thermal conductivity, k, of the near-surface material and the geothermal gradient, dT/dz, i.e.

$$q = k \frac{dT}{dz} . \quad (1)$$

The conductivity can be measured either *in situ* at the location of temperature measurements or by subsequent measurements on material recovered from the seabed, generally provided by gravity or piston cores. *In situ* measurements could be obtained, for example, with a Lister probe (Lister 1979; Hyndman *et al.* 1979) by monitoring and inverting the decay of a calibrated heat pulse. A similar technique is used to yield the thermal conductivity from samples using a needle probe (von Herzen & Maxwell 1959) with corrections for *in situ* conditions (Radcliffe 1960). The temperature gradient is generally derived from a set of *in situ* temperature measurements.

Natural gas hydrates occur worldwide in sediments on continental slopes and insular margins (Kvenvolden 1993). The occurrence of gas hydrates in nature is controlled by an interrelation among the factors of temperature (T), pressure (P) and composition. Because the exact composition of gas and water in sediment pore spaces is normally not known, a pure methane–water system is commonly assumed to predict the depth and temperature regime where naturally occurring gas hydrates are stable (e.g. Claypool & Kaplan 1974; Hyndman *et al.* 1992). The gas hydrate stability zone (HSZ), however, is limited to the upper few hundred metres of the ocean floor, beneath which temperatures are too high for hydrates to exist. In seismic data the base of the hydrate stability zone (BHSZ) is often marked by a bottom-simulating reflector (BSR) if gas hydrates or free gas are present (e.g. Tucholke *et al.* 1977; Shipley *et al.* 1979; Minshull & White 1989; Grevemeyer *et al.* 2000). This reflector follows the shape of the seabed and often cuts across the stratigraphy of sediments. Because the BSR coincides with the phase boundary of gas hydrate stability, its position marks an isotherm. Consequently, knowing the temperature at the seabed, the geothermal gradient could be derived from BSRs (see e.g. Yamano *et al.* 1982; Cande *et al.* 1987; Davis *et al.* 1990; Zwart *et al.* 1996), thus seismically defined BSRs can be used to provide additional constraints on the thermal structure at continental margins.

Nevertheless, there is no general agreement about the temperature at BSR depth. Some authors argue for a pure water–methane system (e.g. Hyndman *et al.* 1992), while others suggest that a seawater–methane system is more likely (e.g. Yamano *et al.* 1982; Davis *et al.* 1990, 1995; Brown & Bangs 1995). In terms of the empirical relationships for a pure water–methane or seawater–methane system, the offset of temperature between both relationships is about 1.1 K (Dickens & Quinby-Hunt 1994; Brown & Bangs 1995). To make things worse, recent drilling results from the Cascadia Margin (Westbrook *et al.* 1994) and the Blake Ridge (Paull *et al.* 1996; Ruppel 1997) indicate that the temperature at BSR depth could be more than 2 K lower than given by the seawater–methane prediction (or >3 K using the pure water–methane system) if the BSR marks the BHSZ.

Another prerequisite for the calculation of heat flow through continental margins is the thermal conductivity of the sediment between the seafloor and the BSR. If drill sites are present, the conductivity can be derived from needle probe measurements on core samples (Hyndman *et al.* 1992; Brown & Bangs 1995). Otherwise, conductivity has to be approximated using velocity–depth profiles from seismic studies and empirical relationships between velocity and conductivity (Yamano *et al.* 1982; Cande *et al.* 1987) or relationships between velocity and porosity on the one hand and porosity and thermal conductivity on the other (Davis *et al.* 1990; Kaul *et al.* 2000). However, measurements taken with heat probes in surficial sediment can be extrapolated downwards (Davis *et al.* 1999). Eq. (1) clearly indicates that the error associated with the calculation of the heat flow is strongly dependent on the assessment of both thermal conductivity and geothermal gradient.

The aim of our study is to assess the quality of heat flow estimates derived from BSRs and to provide a method for the calculation of continental margin thermal properties from this prominent seismic reflector. We therefore used downhole temperature measurements, thermal conductivities, porosities and logging data from Ocean Drilling Program (ODP) legs studying gas-hydrate-bearing sediments. ODP legs 112, 131, 141 and 146 were drilled into the active continental margins of Peru, Nankai (Japan), Chile and Cascadia (British Columbia and Oregon), respectively, while leg 164 investigated the Blake Ridge, a hydrate-bearing portion of the passive continental margin off South Carolina.

RESULTS FROM DRILLING

Since the late eighties 10 ODP sites have been drilled into gas-hydrate-bearing sediments, starting with leg 112 on the Peruvian margin (Suess *et al.* 1988). Safety concerns did not allow drilling through a BSR. Site 688 was therefore drilled at a location where no BSR was seen, although only a few kilometres to the south a seismic survey detected a BSR. At the site, however, gas hydrates were recovered and the holes penetrated well below the hydrate stability field. During leg 131, site 808 was drilled on the Nankai margin off Japan into and below the HSZ (Taira *et al.* 1991). Like site 688, site 808 was at a location where seismic soundings did not indicate a BSR. However, these legs provided evidence that only a small amount of pore space is filled with gas hydrates in the HSZ or with free gas below. As a consequence, sites 859, 860 and 861 of leg 141 on the Chilean Margin (Behrmann *et al.* 1992) were drilled through a BSR. Encouraged by leg 141, sites 889 and 892 of leg 146 offshore Vancouver Island and Oregon, respectively, also penetrated BSRs (Westbrook *et al.* 1994). Two years later, during leg 164 on the Blake Ridge, sites 994, 995 and 997 were again drilled below the BHSZ as revealed by seismic studies and logging (Paull *et al.* 1996). All the data described below have been taken from these drill sites.

Temperature at BSR depth

In situ temperature measurements in ODP drillholes have been made with different tools, that is, an APC (advanced piston corer), WSTP (water sampler, temperature, pressure) and/or DVTP (Davis–Villinger temperature–pressure) tool. ODP's Adara APC tool (Horai & von Herzen 1986; Fisher &

Becker 1993) fits into the cutting shoe of the advanced piston corer. APC data tend to be smoother than the WSTP data because of the greater stability of the data logger, the relative certainty that the APC tool has firmly penetrated into sediments during firing of the hydraulic assembly, and the fact that the tool accumulates data records and reports only averages. Its nominal absolute accuracy is ± 0.1 K. At depths below which the Adara tool can no longer be used, but where the formation is sufficiently competent, the WSTP tool is used instead. WSTP reports only resistance, which must be later converted to temperature using the calibration of the sensor (Fisher & Becker 1993). Its nominal accuracy is ± 0.1–0.2 K. The DVTP is ODP's successor of the WSTP tool. The probe's geometry is nearly cylindrical over a much longer distance than the WSTP so that the DVTP more closely approximates a line source (Davis *et al.* 1997). The tip of the probe is pointed to minimize formation stresses associated with insertion. In addition, the electronics are more stable than those in the WSTP, giving an absolute accuracy of about ± 0.1 K.

Because measurements in the open borehole suffer from circulating fluids, all the tools have in common the fact that they penetrate sediments ahead of the drill bit. After penetration of the sensors, they record a pulse of frictional heating, which decays while the tools remain for 10–15 min in the formation. The calculation of equilibrium temperatures follows the same procedure for all instruments. The extrapolation of the frictional heating pulse to equilibrium temperature generally accounts for the nominal uncertainty of ~ 0.1 K. The instruments themselves generally have a resolution of about 0.01 K. The overall uncertainty, however, can be much larger if microfractures created during insertion allow cold sea water circulation close to the sensor or if the probe does not remain stationary during the measurement period (Hyndman *et al.* 1987).

During several ODP legs, the different tools have been used at the same hole or site, which allows a calibration of the tools against each other. For example, at sites 995 and 997 all three tools were deployed (Paull *et al.* 1996) and at hole 889 A the Adara and WSTP tools were used (Westbrook *et al.* 1994). Generally, temperatures measured with different tools in a single hole show a linear temperature increase with depth, suggesting that there is no systematic error associated with any of the tools used. At site 892, however, WSTP and CORK measurements provided different temperature profiles, which could not easily be explained, but may indicate a contemporary fluid flow 'event' (Davis *et al.* 1995). This idea is supported by aqueous flux measurements within the cold seep region close to site 892, which indicate a high degree of variability, with extended periods of downflow and reversals of flow direction over periods of weeks to months (Tryon *et al.* 1999). In our study we used the CORK data, because they seem to represent the most stable regime (Davis *et al.* 1995).

On the Peruvian margin site 688 was drilled only a few kilometres off a seismic profile where a BSR was detected. Using seismic constraints (Pecher 1995) the BSR is located at 400 ± 10 mbsf (metres below seafloor). Only at one location was the temperature measured with the APC (Suess *et al.* 1988). However, during pore-water sampling a second value was obtained in the open borehole. We approximated the gradient for all sites by a linear regression (we discuss the reason for the linear approach below). Along with the bottom water temperature from oceanographic data, a linear gradient of ~ 51.6 K km^{-1} was obtained (Fig. 1). Because this is consistent with surface measurements using heat probes (Yamano & Uyeda 1990) we consider the gradient as reliable. The temperature at BSR depth is 22.3 °C, thus 1.3 K lower than the prediction from the seawater–methane system (Figs 1 and 2).

Off Japan on the Nankai margin, site 808 was drilled during ODP leg 131. A BSR was observed about 2 km landward of the site, although at a shallower depth. Hyndman *et al.* (1992) approximated the depth of the BHSZ as 205 ± 7 mbsf. WSTP data have been obtained at the site (Taira *et al.* 1991). Linear regression gave a temperature at the BHSZ that is 0.6 K higher than the prediction of the seawater–methane hydrate stability, i.e. the temperature is 25.8 °C.

ODP sites 859, 860 and 861 of leg 141 were drilled close to the Chile triple junction and were chosen to study the effects of the subduction of a seafloor spreading centre. The sites are between 3 and 17 km away from the deformation front (Behrmann *et al.* 1992; Brown & Bangs 1995). At site 859 the location of the BSR could be derived from logging data indicating a low-velocity zone at 97 mbsf (Bangs *et al.* 1993). At site 860 the BSR was proposed to occur at $\sim 200 \pm 10$ mbsf (Brown & Bangs 1995). However, sonic logging detected a low-velocity layer at 158 mbsf (Behrmann *et al.* 1992) that may have a free gas layer and hence maybe the BHSZ. Logging data at site 860, however, are likely to be somewhat spurious. At site 861 the depth has to be approximated using seismic reflection data (Brown & Bangs 1995). The BSR occurs at 250 ± 10 mbsf. Adara APC and WSTP data are available at all sites. Site 859 did not provide a linear gradient. The non-linear profile from site 859 suggests fluid expulsion close to the deformation front. However, a measurement was taken at BSR depth, indicating a temperature of 19.6 °C, about 0.9 K lower than the temperature derived from the seawater–methane curve. At site 860 data are only available in the uppermost section of the hole. Linear extrapolation of measured temperatures yields consistent BSR temperatures when a BSR depth of 158 mbsf is assumed as suggested by logs. The seismically derived BSR depth of 200 mbsf results in a large temperature difference, therefore assuming a depth of 158 mbsf seems to be more plausible. Site 861 provided a linear geothermal gradient down to BSR depth, and the temperature of 17.5 °C is in reasonably good agreement with the seawater–methane relationship for gas hydrate stability.

During leg 146, site 889 was drilled into the continental margin off Vancouver Island and site 892 was drilled on an accretionary ridge off Oregon. Adara APC and WSTP data are available from site 889 and the BSR was defined by logging and vertical seismic profiling (VSP) data (Westbrook *et al.* 1994; MacKay *et al.* 1994). The temperature data indicate a linear gradient. At BSR depth the temperature of 14.5 °C is about 0.8 K lower than expected assuming the seawater–methane relationship. The CORK data from site 892 provided a similar trend (Davis *et al.* 1995). An abrupt transition in velocity derived from a VSP experiment was determined in hole 892C at 72 mbsf (Westbrook *et al.* 1994; MacKey *et al.* 1994), which is about 8 m shallower than estimated from the (regional) BSR observed in seismic records. Assuming that the velocity anomaly at 72 mbsf marks the BHSZ, the temperature is ~ 0.1 K lower than the prediction of the seawater–methane model.

Drilling on the Blake Ridge during leg 164 provided three sites that were drilled through the BHSZ. At sites 994, 995 and 997 logging constrained free gas below the HSZ (Paull *et al.* 1996). The BHSZ occurs at 429, 450 and 451 mbsf, respectively.

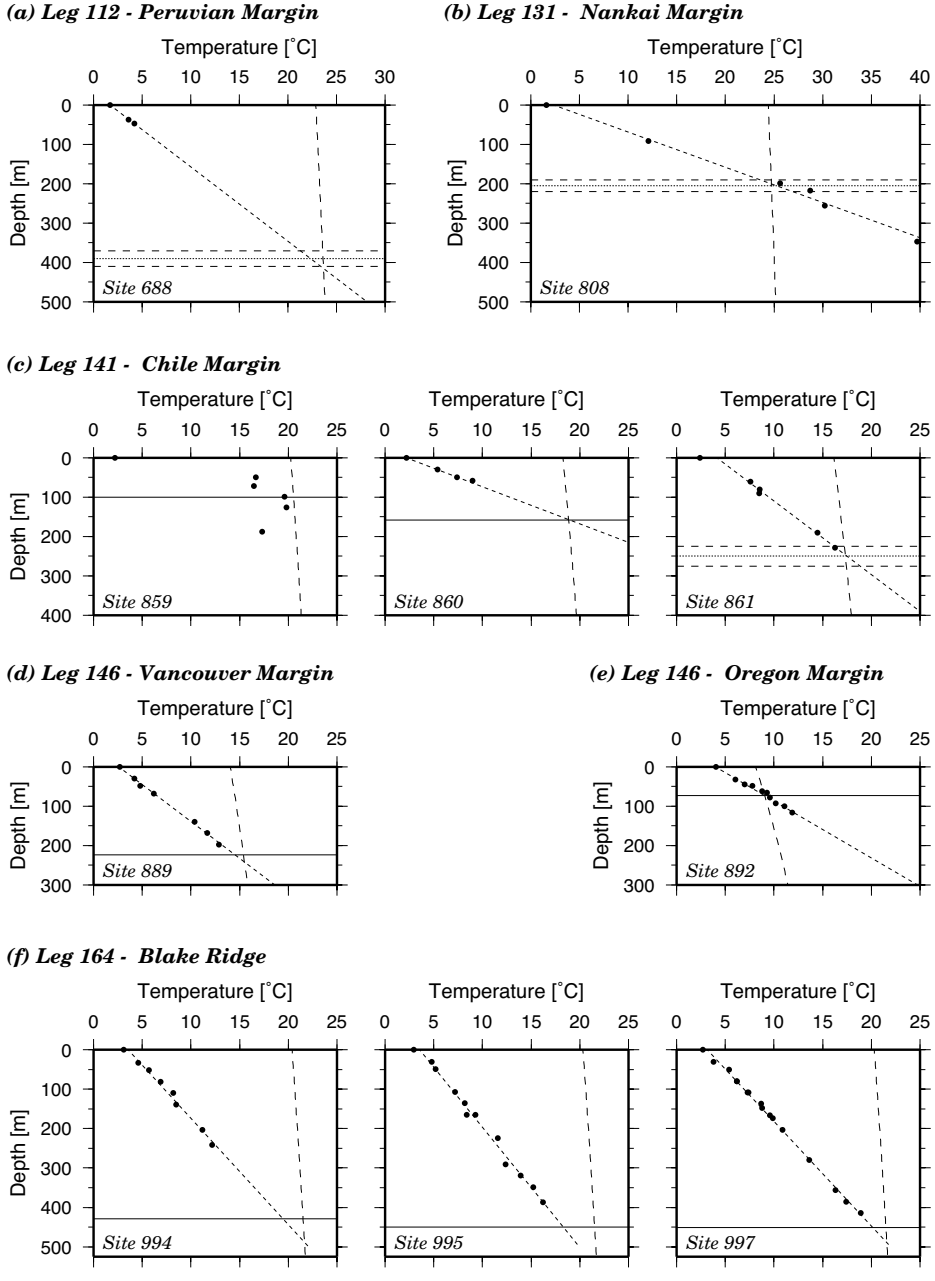

Figure 1. Downhole temperature measurements in gas-hydrate-bearing sediments. If the base of the hydrate field was derived by downhole measurements such as sonic logs, the BSR is marked by a horizontal solid line; if the BSR depth was derived from seismic reflection data, the BSR is marked by a horizontal dotted line and its uncertainty is given by the broken lines. Linear temperature gradients have been obtained by a least-squares fit. The vertical broken line is the prediction from a seawater–methane system (Brown & Bangs 1995). Data are from ODP legs 112 (Suess *et al.* 1988), 131 (Taira *et al.* 1991), 141 (Behrmann *et al.* 1992), 146 (Westbrook *et al.* 1994; Davis *et al.* 1995) and 164 (Paull *et al.* 1996). See text for further description.

In situ temperature measurements have been made with the Adara APC, the WSTP and the DVTP tools (Paull *et al.* 1996; Ruppel 1997). With respect to the seawater–methane curve, the best-fitting linear gradients indicate temperatures that are 1.3–3.2 K too low. Temperatures for sites 994, 995 and 997 at BSR depth are 19.5, 18.3 and 20.2 °C, respectively.

Fig. 2 shows all the reliable temperatures at BSR depth derived from downhole measurements. It is important to note that seven out of 10 values for the temperature at the BSR are below the seawater–methane prediction for the BHSZ (Dickens & Quinby-Hunt 1994; Brown & Bangs 1995).

Temperature at the seafloor

To find the geothermal gradient from the BSR, the temperature at the seafloor is required, which can be taken from oceanographic measurements. However, seasonal variations may affect the temperature of the bottom water at continental margins (e.g. Ruppel *et al.* 1995; Kaul *et al.* 2000). In this case, the seafloor temperature will be a function of unknown behaviour and the uppermost temperature gradient will be disturbed. Generally, the shallow-water regions are prone to transient bottom water temperatures. The impact of such

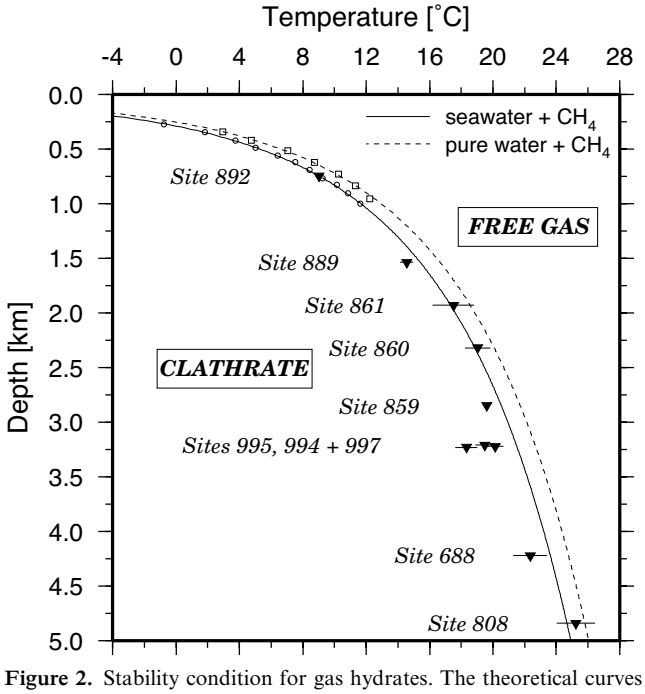

Figure 2. Stability condition for gas hydrates. The theoretical curves for a pure water–methane and seawater–methane system are from Brown & Bangs (1995). Open symbols are laboratory measurements from Dickens & Quinby-Hunt (1994). Triangles are temperatures at BSR depth derived from the regression of downhole measurements shown in Fig. 1 and summarized in Table 1.

seasonal variations is visible in Fig. 1; for example, the bottom water temperature at sites 861, 994, 995 and 997 is 0.45–1.7 K lower than the seafloor temperature, consistent with the linear gradient derived from downhole measurements. Therefore, either a time-series of bottom water temperatures or measurements with heat probes are required to correct the transient effects of subsurface temperatures (Ruppel *et al*. 1995). In the following analyses and discussion, we will use as seafloor temperature the reference temperature taken with the downhole tools on or close to the seabed.

Geothermal gradient from BSR depth

The geothermal gradient dT/dz is calculated from the difference between the temperature at the BSR and that at the seabed, divided by the subseafloor depth of the BSR. To assess the errors in gradients obtained from BSRs we used a water–methane system and a seawater–methane system. All data have been compared to the best-fitting gradient from downhole measurements. Table 1 summarizes the results. Errors for the pure water–methane model range from 5 to 25 per cent and are therefore higher than the errors of 5–20 per cent for the seawater–methane system. It is important to note that in the cases studied here individual errors due to seasonal variations in the bottom water temperatures could be up to $\sim$10 per cent. In other areas the error might be even higher. However, using a seafloor temperature derived from the best-fitting linear gradient instead of the measured seafloor temperature, the error for site 861, for example, decreases from 10 per cent to only 1–2 per cent, suggesting that an appropriate correction for the bottom water temperature increases the quality of estimates significantly.

Thermal conductivity from needle probe measurements

Thermal conductivities on ODP drill cores are measured routinely with a needle probe system (von Herzen & Maxwell 1959). Normally the needle is inserted perpendicular to the core axis. In the case of anisotropy parallel to bedding, the measurement is affected by this anisotropy and the results will be biased (Pribnow *et al*. 2000; see Discussion below). Fig. 3 shows the thermal conductivity of sites from legs 112, 131, 141, 146 and 164 as a function of depth. Values are widely scattered. Some of the laboratory core measurements may be biased and systematically in error. In general, however, measurements on cores and *in situ* measurements with a Lister probe yielded similar values within the error bounds of the estimates (e.g. Davis *et al*. 1990, 1999; Pribnow *et al*. 2000). Moreover, the values support a common trend of increasing values with depth. The scatter may therefore arise from microfractures in the drill core, which will affect the measurements, or from variations in the composition of the sediment. Generally, the conductivity of an n-component system is given by

$$k = \prod_{i=1}^{n} k_i^{v_i}, \tag{2}$$

where k_i is the conductivity of the ith component and v_i is its volume per cent. Thus, variations in the composition or in the abundance of a material with a specific conductivity produce a change in the measured conductivity. These variations could occur everywhere, but may be most prominent in turbidites. Nevertheless, the conductivity of surficial sediments is dominated by the water content of the sediment and hence porosity, and thus has often been described by a two-component system

Table 1. Comparison of temperatures at BSR depth and geothermal gradients derived from ODP drill sites and models for gas hydrate stability.

Site	688	808	859	860	861	889	892	994	995	997
Water depth (m)	4220	4841	2850	2320	1928	1535	748	3210	3230	3220
BSR depth	400	205	97	158	250	224	72	429	450	451
T_0 (°C)	1.7	1.6	2.2	2.2	2.4	2.7	4.05	3.1	2.9	2.7
T_0 from dT/dz	1.69	2.36	–	2.21	4.14	2.58	3.98	3.55	3.52	3.15
T_{BSR}	22.34	25.23	19.63	19.02	17.5	14.55	9.01	19.48	18.32	20.15
T_{BSR} pure water–methane	24.77	25.8	21.72	20.67	18.57	16.68	10.37	22.66	22.7	22.68
T_{BSR} seawater–methane	23.62	24.67	20.53	18.86	17.33	15.37	9.06	21.48	21.53	21.5
dT/dz (K km^{-1})	51.62	111.6	–	106.4	53.5	53.4	69.4	37.1	32.9	37.7
dT/dz pure water–methane	57.7	118.1	202.3	116.9	64.7	62.4	87.2	45.6	44.0	44.3
dT/dz seawater–methane	54.8	112.5	189.9	105.4	59.7	56.6	69.1	42.8	41.4	41.7

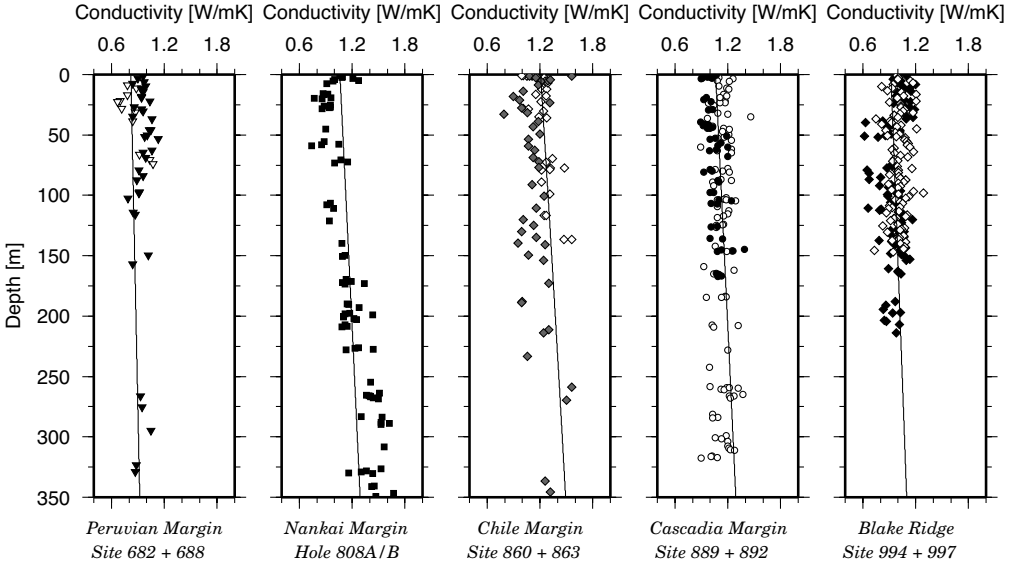

Figure 3. Thermal conductivity as a function of depth. Data are from needle probe measurements on ODP core samples. The trends plotted have been calculated from eq. (3) and the Athy's law porosity profiles shown in Fig. 4 and Table 2 (data sources: Suess *et al.* 1988; Taira *et al.* 1991; Behrmann *et al.* 1992; Westbrook *et al.* 1994; Paull *et al.* 1996).

of water and a matrix material (Davis *et al.* 1990; Villinger *et al.* 1994). Its conductivity is given by

$$k = k_{\mathrm{w}}^{\phi} k_{\mathrm{g}}^{1-\phi}, \tag{3}$$

where k_{w} is the conductivity of water, k_{g} is the conductivity of the matrix (geometric mean) and ϕ is the porosity. Brigaud & Vasseur (1989) suggested that this model should be applied to individual vertical lithological units identified in drill sites. Unfortunately, the required data are not available for most survey areas. However, it was shown in several studies that the same model provided a reasonably good approximation for the uppermost 500–1000 m of marine sediments (e.g. Davis *et al.* 1990, 1999; Villinger *et al.* 1994). Fig. 4 shows the porosity from the drill sites shown in Fig. 3 and Fig. 5 shows the conductivity as a function of porosity. Also shown are models calculated from eq. (3) using a binary mixture (water + sediment) with a conductivity of water of $k_{\mathrm{w}} = 0.6$ W m^{-1} K^{-1} and k_{g} values of 1.5, 2.5 and 3.5 W m^{-1} K^{-1}. A value of $k_{\mathrm{g}} = 2.5 \pm 0.1$ W m^{-1} K^{-1} produced a reasonably good fit to all data and is in agreement with previous estimates for marine sediments (e.g. Davis *et al.* 1990; Villinger *et al.* 1994). In Fig. 4 and Table 2, we show Athy's law porosity–depth relationships (Athy 1930) fitted to measured porosities and in Fig. 3 we show the thermal conductivity calculated from eq. (3) and the same functions. The fit to the measured data provided an rms error of 0.12–0.17 W m^{-1} K^{-1}. Histograms calculated from all conductivity values (Fig. 6) may suggest that, at least for the Peruvian and Cascadia margins and the Blake Ridge, a mean value for the conductivity provides almost the same fit; the

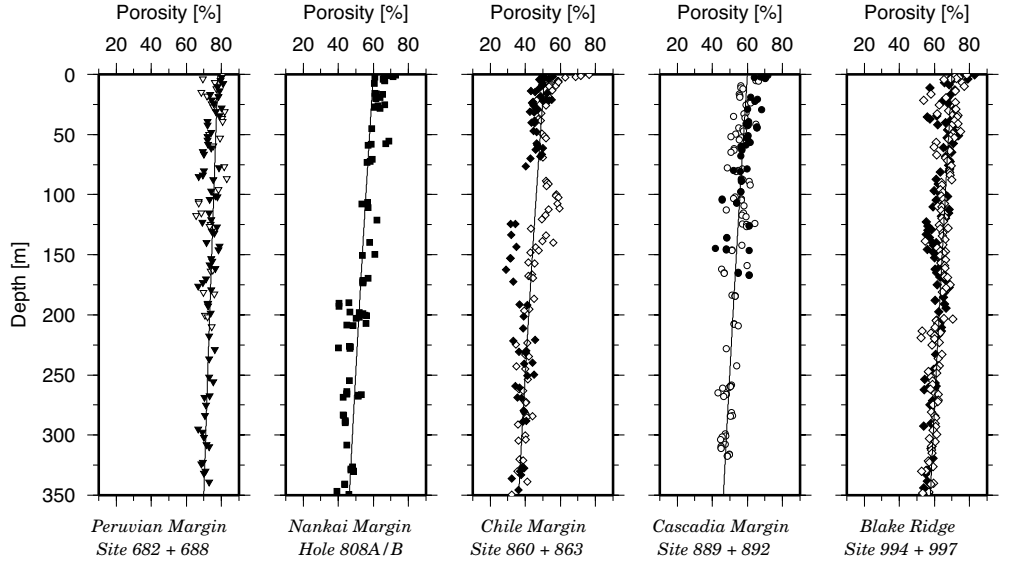

Figure 4. Porosity as a function of depth. The solid lines are Athy's law functions (Table 2) fitted to the ODP core data (same data sources as in Fig. 3).

Table 2. Assessment of thermal conductivity in ODP drill sites.

Location	Athy's porosity*		Average conductivity (W m^{-1} K^{-1})	Rms conductivity error derived from	
	a_1 (%)	a_2 (m)		porosity model	mean value
Peru	78	3200	0.85	0.124	0.117
Nankai	60	1350	1.05	0.172	0.263
Chile	51	1020	1.25	0.17	0.183
Cascadia	60	1350	1.1	0.119	0.11
Blake Ridge	70	1800	1.0	0.14	0.132

* $\phi = a_1 \exp(-\text{depth}/a_2)$

rms error for mean values is 0.11–0.18 W m^{-1} K^{-1} (Table 2). Only for the Nankai Margin does the histogram display two peaks with different conductivities (Figs 5 and 6). The second peak, however, is from material recovered well below the BHSZ. Nevertheless, using only material from the upper sequence the fit is still much worse, increasing from 0.17 to 0.26 W m^{-1} K^{-1}.

In situ thermal conductivity of gas-hydrate-bearing sediment

The presence of hydrate will have some effect on the conductivity. Stoll & Bryan (1979) found a thermal conductivity for propane hydrate measured in the laboratory of 0.394 W m^{-1} K, a decrease of about 35 per cent compared to water. At normal sediment porosities, the effect on the bulk thermal conductivity will be less than this, but will probably still be significant. We therefore try to assess the effect of gas hydrate by calculating *in situ* conductivities using a three-component system composed of hydrate, matrix material and open void spaces filled with water. Quantities have been derived from site 995 drilled on the Blake Ridge. We closely follow Guerin *et al.* (1999) in calculating porosities and hydrate saturation of the sediment.

Because the neutron porosity and the density logs from leg 164 are of poor quality, the most reliable porosity estimation may be derived from the resistivity log (Fig. 7), which is commonly the least sensitive log to poor hole conditions. Generally Archie's law (Archie 1942) has routinely been used by logging scientists to give the porosity structure of sediments from resistivity data. Recently, this technique has been brought into question. Spangenberg (2000) argued that the prediction of Archie's law in hydrate-bearing sediments could be biased. This is because the hydrate does not seem to form a cement in the same way as quartz or calcite does, but rather occupies pore bodies. However, there is no experimental proof of these results, and concentrations of gas hydrates derived from Archie's law (e.g. Paull *et al.* 1996; Collett & Ladd 2000) are in good agreement with values obtained from geochemical studies on sediment samples recovered during leg 164 on the Blake Ridge (Dickens *et al.* 1997; Matsumoto & Borowski 2000). Thus,

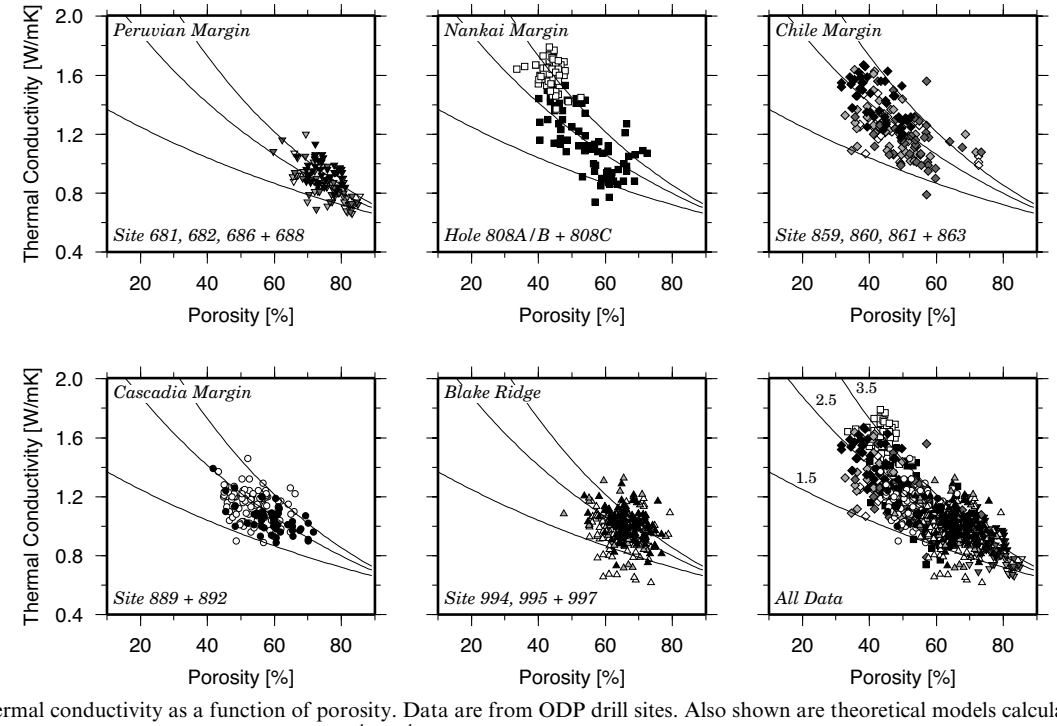

Figure 5. Thermal conductivity as a function of porosity. Data are from ODP drill sites. Also shown are theoretical models calculated from eq. (3) using matrix conductivities of 1.5, 2.5 and 3.5 W m^{-1} K^{-1}, respectively (same data sources as in Fig. 3).

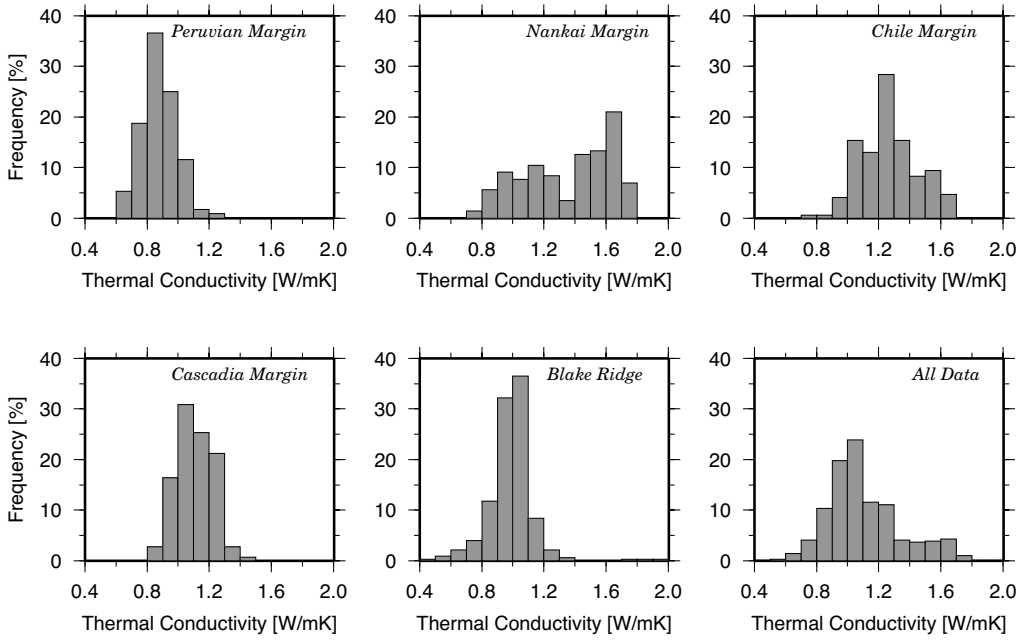

Figure 6. Histograms of thermal conductivity calculated from needle probe measurements on ODP core samples (same data sources as in Fig. 3).

to provide an initial assessment it seems reasonable to follow Guerin *et al.* (1999) in calculating porosities and hydrate saturation of the sediment from Archie's law.

In terms of Archie (1942), an empirical relationship between porosity ϕ, the measured resistivity R_t and the pore water resistivity R_w in sandy formations is given by

$$\phi = \left(a \frac{R_w}{R_t} \right)^{1/m}, \tag{4}$$

where m and a are two empirical parameters derived from cross-correlation between log resistivity and measurements of the porosity on core samples from the same formation. Paull *et al.* (1996) calculated the values to be 0.9 and 2.7, respectively. The resistivity of seawater is given by an empirical formula depending on temperature and salinity,

$$R_w = R_0 \frac{(T_0 + 21.5)}{(T + 21.5)}, \tag{5}$$

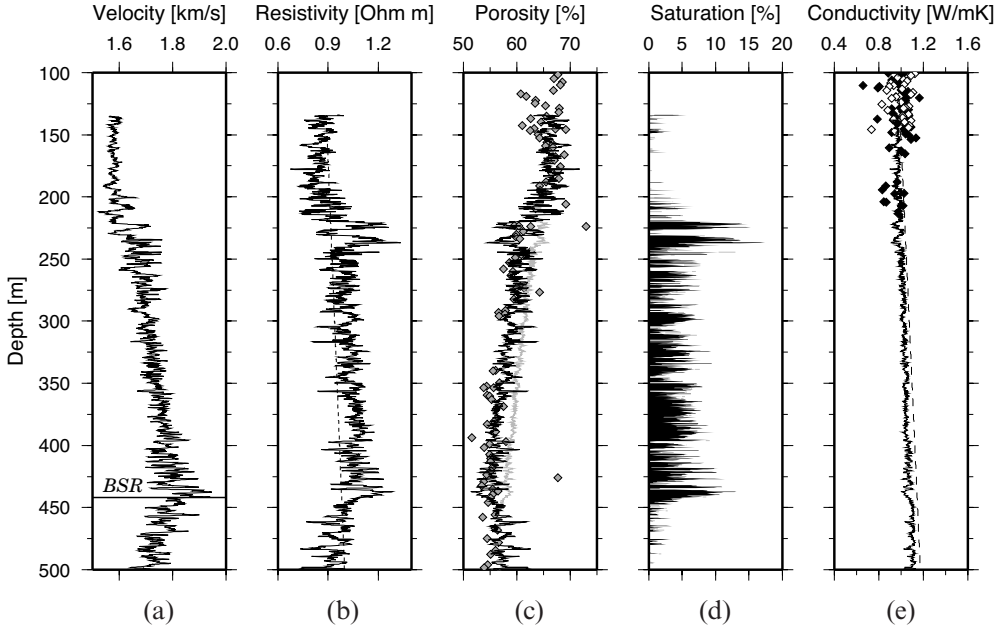

Figure 7. Calculation of the *in situ* conductivity of a three-component system of matrix material, low-conductivity hydrate and open pore spaces filled with seawater. The required parameters have been calculated from logging data obtained at ODP site 995 (Paull *et al.* 1996; Guerin *et al.* 1999). See text for further description. (a) Sonic log data showing BSR depth, (b) resistivity log and background reference model, (c) porosity from resistivity log (black line) and porosity corrected for the amount of hydrate affecting the resistivity log (grey line), (d) hydrate saturation from resistivity log, and (e) calculated *in situ* conductivity (solid line) and conductivity calculated from eq. (3) and Athy's law porosity (Table 2). Symbols are data from ODP core samples (Paull *et al.* 1996).

where $R_0 = 0.240\ \Omega$ m is the resistivity of seawater at a reference temperature of $T_0 = 18\ ^\circ$C (Guerin *et al.* 1999). The temperature is assumed to follow the linear gradient given in Fig. 1. The resulting porosity log is shown in Fig. 7, where it compares well with the porosity estimates on core samples.

Assuming that the higher resistivity observed above the BSR (Fig. 7) is caused by the presence of electrically resistive gas hydrates, the fractional saturation in pore space S can be expressed by (Paull *et al.* 1996; Collett & Ladd 2000)

$$S = 1 - \left(\frac{R_0}{R_t}\right)^{1/n}. \quad (6)$$

It is, however, considered that the resistivity of water-saturated sediments R_0 can be considered as a baseline function of depth, and was approximated by $R_0 = 0.8495 + 2.986 \times 10^{-4} z$ (Paull *et al.* 1996). Laboratory experiments on hydrate sediments yielded a value of $n = 1.9386$. More details on this method are given by Paull *et al.* (1996) and Collett & Ladd (2000). The resulting saturation is between 5 and 15 per cent. Assuming that hydrate increases the resistivity only by occupying part of the pore space, the porosity calculated from the resistivity log has to be corrected by $\phi_c = \phi/(1-S)$. The fit of the corrected porosity to the porosity from core samples is much worse (Fig. 7); however, we have to bear in mind that hydrates vanish upon recovery. Constraints from oxygen isotopic fraction, $\delta^{18}O$ and Cl^- anomalies of pore waters from Blake Ridge drill sites (Dickens *et al.* 1997; Matsumoto & Borowski 2000) generally gave a saturation systematically lower than the assessment from logging. Therefore, the calculated saturation is a maximum value.

We are now able to calculate *in situ* conductivities assuming a three-component system. We used conductivities of 0.6, 0.4 and 2.5 W m^{-1} K^{-1} for water, gas hydrate and sediment matrix, respectively. The resulting conductivity profile is shown in Fig. 7. Although gas hydrate reduces the bulk conductivity compared to the profile calculated from Athy's law, the values are only insignificantly lower and therefore still within the typical uncertainty of estimates from needle probes. In addition, we have to bear in mind that the calculated saturation was a maximum value; thus, gas hydrate has only a small and therefore insignificant influence on the bulk thermal conductivity, and hence on the heat flow.

Thermal conductivity from seismic data

Compared to seismic studies and their coverage of continental slopes, scientific or industry drill sites sample only a few locations. Consequently, it is often not possible to use constraints from drilling to assess the thermal conductivity of slope sediments. In this case, two different techniques have generally been used. First, conductivity has been calculated directly from seismic velocities (e.g. Yamano *et al.* 1982; Cande *et al.* 1987) using an empirical relationship between velocity and conductivity (Horai 1981). Second, seismic velocity has been transformed first to porosity and then porosity to thermal conductivity using eq. (3) (e.g. Davis *et al.* 1990; Kaul *et al.* 2000). However, the relationship between seismic velocity and porosity is not unique. Because porosity is an important factor governing the thermal conductivity of unconsolidated marine sediments, the same may hold for velocity and conductivity. To obtain the errors associated with both approaches we used logging data from ODP legs 141, 146 and 164 to assess the relationship between velocity and porosity, and hence conductivity. Velocity was measured directly while porosity was calculated again from resistivity logs using Archie's (1942) law.

Although the velocity–porosity data shown in Fig. 8 have some overlap, it is evident that different settings generally show an individual trend. A global relationship derived by Erickson & Jarrard (1998) provides a surprisingly poor overall fit to the data (Fig. 8a). Errors in porosity derived from their relationship for unconsolidated sediment could be as high as 4–7 per cent for the Cascadia data and 10–15 per cent for the Blake Ridge data. The local relationship from Davis & Villinger (1992) provided a good fit, at least for the data from leg 146. However, it was calculated for turbidites derived from the Cascadia Margin, that is, from the same source area. Therefore, velocities

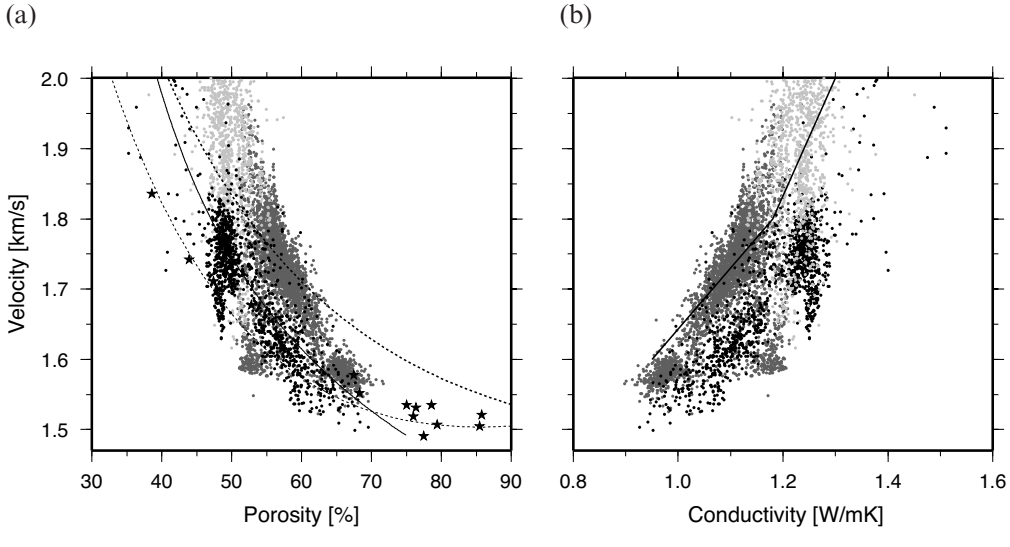

Figure 8. (a) Sonic velocity versus porosity calculated from resistivity logs. Also shown are global velocity–porosity relationships (broken line) of unconsolidated sediment (Erickson & Jarrard 1998) and a relationship (solid line) derived for Cascadia (Davis & Villinger 1992). Black, grey and light grey dots are logging data from ODP site 859, 889 and 995, respectively. Stars are values from the study of Hamilton (1971). (b) Sonic velocity versus conductivity calculated from porosity and eq. (3). Also shown is the relationship derived by Horai (1981).

have to be converted carefully into porosities. The same holds for the velocity–conductivity trend from Horai (1981). The function was derived primarily from data of Deep Sea Drilling Project (DSDP) leg 60 and may therefore provide a good fit for data from offshore Japan. The fit to the data from leg 164 is fair, but the overall fit is less promising (Fig. 8b); errors of 0.2–0.3 W m^{-1} K^{-1} are common and hence errors of 20–30 per cent in heat flow calculations.

DISCUSSION

Geothermal gradient

The calculated temperature gradient obtained from seismically detected BSRs depends on temperatures at the seafloor and BSR. A two-point approximation of the geotherm is generally very simplistic and is only appropriate for homogeneous sediments with a constant thermal conductivity. Simple calculations show that geotherms calculated on the basis of a constant thermal conductivity and porosity-derived conductivities differ down to BSR depth by the order of 0.1 K. These differences cannot be resolved using the downhole tools available (see previous chapter). Therefore, a linear approximation of the geotherm is applicable for most settings and a constant thermal conductivity is appropriate for most BSR-derived heat flow studies. However, environments characterize by fluid flow, like site 859 drilled close to the deformation front at the Chilean Margin, provide a non-linear temperature profile and have to be analysed carefully.

Despite these assumptions concerning the geotherm, the main error may arise from the temperature at the BHSZ. The compilation of temperatures at BSR depth suggests that seven out of 10 assessments give values up to $\sim$3 K lower than expected from the stability of gas hydrate in a system dominated by seawater and methane (Brown & Bangs 1995; Dickens & Quinby-Hunt 1994). On average, the temperature was 0.9 K too low. Current models for the formation of gas hydrates in marine sediments generally assume that the phase equilibria of a bulk water and gas mixture measured in the laboratory can be applied directly to nature. However, laboratory tests do not cover the whole range of pressures found in the natural environment and generally do not account for the effects of host-sediment properties on hydrate stability (Clennell *et al.* 1999). Moreover, there are no laboratory values available for a seawater–methane system at depths greater than about 1000 m, and it is assumed that there is a deviation of $\sim$1.1 K to the pure water–methane system (Dickens & Quinby-Hunt 1994; Brown & Bangs 1995), which is supported by laboratory data down to 7000 m (Sloan 1990). Therefore, uncertainty in the stability curves at high pressure renders a precise interpretation of the temperature disparity (Wood & Ruppel 2000). However, in general, statistical thermodynamic calculations show similar trends (Englezos & Bishnoi 1988; Tohidi *et al.* 1995), although the model of Tohidi *et al.* (1995) yields dissociation temperatures much closer to those determined for the Blake Ridge BSR. Nonetheless, there is still a discrepancy between the prediction and the temperatures provided by downhole measurements. In addition, drilling on the Blake Ridge gave variations in temperature of $\sim$2 K between sites 994, 995 and 997. These sites are only 4–10 km apart and the BHSZ occurs at roughly the same depth. Consequently, processes other than P/T conditions may act on the stability of gas hydrates.

Ruppel (1997) and Hovland *et al.* (1997) found differences between the depth of the BSR and the theoretical depth of the BHSZ. They associated this discrepancy with capillary forces arising in fine-grained sediments, such as montmorillonite-rich sediments on Blake Ridge. These forces may inhibit gas hydrate formation. Recent work (Clennell *et al.* 1999) and laboratory measurements (Handa & Stupin 1992; Zakrzewski & Handa 1993) indicate that capillary forces in fine-grained materials may depress dissociation temperatures by 0.5–8 K. Thus, supercooling due to capillary inhibition of gas hydrate stability could account for the lower temperatures at BSR depth (Ruppel 1997). In addition, elastic properties in the drill sites suggest that there is a coexistence of hydrates and free gas beneath the BSR. Guerin *et al.* (1999) suggested that again capillary effect could explain this unexpected phenomenon. However, using constraints from drilling on the Blake Ridge, the thermodynamic calculations of Henry *et al.* (1999) showed that additional inhibition forces other than pore size effects must be involved to explain the temperature shift as an equilibrium phenomenon. Henry *et al.* therefore suggested that the BSR may lie at non-equilibrium P/T conditions. Ruppel (1997) suspected that the Blake Ridge may still suffer from incomplete readjustment in response to upper Pleistocene–Holocene climate change. Nevertheless, the occurrence of the BSR at an overly shallow depth cannot be easily explained by realistic combinations of pressure-driven deepening (sea-level rise) and temperature-driven shoaling (bottom water temperature changes). Equilibration may also be limited by diffusional transport of gas, water and salt components (Henry *et al.* 1999) or be perturbed by significant flows of fluid or heat through the sediments or along buried faults (Wood & Ruppel 2000).

Most of the processes discussed so far reduce the temperature at the BSR. Chemical impurities, however, can increase the temperature as well. Methane hydrate stability is promoted very strongly by the presence of even small amounts of ethane, carbon dioxide, hydrogen sulphide and higher hydrocarbons. For example, 1 per cent ethane would counterbalance the effect of the seawater inhibition (Clennell *et al.* 1999). In addition, the capillary model of Henry *et al.* (1999) indicates that where free gas is present at the BSR, the temperature could be too warm (B. Clennell, personal communication, 2000).

These factors have important implications for the calculation and accuracy of geothermal gradients from BSRs. First, even when natural gas hydrate stability is related to a seawater–methane system, temperatures at BSR depth could be incorrect by up to 4 K, or possibly even higher. Resulting errors may be up to 20–30 per cent, although they depend strongly on the local features. Second, even if drilling provided temperatures at BSR depth, the local variability at the Blake Ridge indicates that temperature may vary by $\sim$2 K on a local scale; errors might be as high as 20 per cent. If, in addition, the temperature at the seabed is affected by seasonal variations, the error of the geothermal gradient may reach 40 per cent. Consequently, we have to emphasize the fact that geothermal gradients derived from BSRs alone might be tenuous. This clearly contradicts previous claims, suggesting that errors arising from P/T conditions and from seafloor temperatures are small (Yamano *et al.* 1982; Cande *et al.* 1987) and the error of $\sim$25 per cent in the assessment of heat flow from seismic BSRs is primarily controlled by the estimation of thermal conductivity.

Errors, however, can be reduced if geothermal gradients from heat probe measurements are available and are used to

calibrate the temperature at BSR depth. Sometimes, though, measurements with heat probes have to be corrected for high sedimentation rates (e.g. Kaul *et al.* 2000) or transient features due to variable bottom water temperatures (e.g. Ruppel *et al.* 1995). Moreover, in regions where dewatering of accretionary wedges occurs, heat probes may not measure the pure conductive heat loss, but could be affected by advective heat transport (Davis *et al.* 1990). In this case, the benefit from traditional geothermal studies might be minor.

Conductivity of slope sediments

Modern heat flow measurements with a Lister probe (Lister 1979; Hyndman *et al.* 1979) provide *in situ* conductivity measurements at the same depth as where *in situ* temperatures have been measured to obtain the geothermal gradient. Both data sets are inverted jointly to yield the heat flow (e.g. Villinger & Davis 1987). BSR-derived heat flow is based on data distributed quite differently. Temperatures are taken at the seafloor and at BSR depth. To find the heat flow, the thermal conductivity structure between both data points must be known. In general, the information required has not been measured, thus we have to infer thermal conductivities. Where drilling did not provide the appropriate data, most studies used empirical relationships between seismic velocities, porosity and thermal conductivity. As shown above, the benefits from such relationships are generally tenuous and they may give errors that are too large for a reasonable heat flow survey. Based on the following arguments, we recommend the use of measurements from surficial sediments instead where neither scientific nor industry drill sites are available.

Fig. 5 shows the relationship between conductivity from needle probes and porosity. Because porosity generally decreases with depth (Fig. 4 and Table 2), conductivity increases with depth. This fact is shown in Fig. 3. However, as shown above, the rms error of needle probe measurements with respect to a porosity-dependent model and to a mean value is more or less the same. Moreover, if anisotropy is present, needle probes do not measure the vertical conductivity that governs the heat flow, but a value also affected by the horizontal conductivity. Pribnow *et al.* (2000) have shown that on the eastern flank of the Juan de Fuca Ridge, anisotropy increases with depth, with the higher component being along the layering while the vertical component remains nearly constant. Thus, it might be reasonable to hypothesize that the increase of the bulk conductivity with depth is primarily related to the increasing horizontal component of conductivity. Because we believe that anisotropy is a global phenomenon in margin sediments, we assumed that thermal conductivity remains (within its error bounds) constant in the uppermost few hundred metres of sediment. This idea is supported by the linear trend generally visible in downhole measurements (Fig. 1); gradients would only show curvature in the case of a strong depth dependence of vertical conductivity, or if vertical advection occurs.

This fact may suggest that it might be appropriate to use conductivity from *in situ* measurements with a Lister probe (Hyndman *et al.* 1979) or from needle probe measurements on gravity or piston cores (von Herzen & Maxwell 1959), rather than using relationships between seismic velocity and conductivity or velocity and porosity. This approach might be the best to assess the local variability of thermal conductivity. Generally, there is a good agreement between measurements of near-seabed conductivity and results from drilling. For example, Yamano & Uyeda (1990) measured a conductivity of 0.82 W m^{-1} K^{-1} on piston cores from the Peruvian Margin and drilling gave a mean value of 0.85 W m^{-1} K^{-1} (Fig. 6 and Table 2). Ruppel *et al.* (1995) determined a conductivity of 1.02 W m^{-1} K^{-1} from surficial sediments of the Blake Ridge; leg 164 provided a mean value of 1.0 W m^{-1} K^{-1}. However, Davis *et al.* (1990) found considerable local scatter on the Cascadia Margin, although it clearly falls into two groups—lower values (0.85–0.95 W m^{-1} K^{-1}) in small troughs and in minor slope basins and higher values (1.05 to over 1.2 W m^{-1} K^{-1}) elsewhere. The higher values are consistent with conductivities from ODP drill sites. The difference probably reflects local differences in sediment lithology penetrated. Variations that are consistent with the differences observed in conductivity are seen in 3.5 kHz profiles. Consequently, the assessment of thermal conductivities for the calculation of heat flow from BSRs needs careful inspection of seismic recordings and measured thermal conductivities.

Uncertainty of heat flow estimates

The data analysis and discussion clearly suggest that the assessment of BSR-derived heat flow through continental margins is inherently related to the information available. The calculation of heat flow, as expressed by formula (1), depends on both the geothermal gradient and thermal conductivity. The resulting error is therefore the sum of errors associated with the determination of the thermal gradient and the thermal conductivity structure between the seafloor and the BSR. Table 3 briefly summarizes the errors found in this paper. Clearly, our considerations indicate that previous estimates of possible errors/uncertainties have been far to optimistic (Yamano *et al.* 1982; Cande *et al.* 1987; Kaul *et al.* 2000). In addition, we note

Table 3. Summary of errors associated with the assessment of BSR-derived heat flow values.

Property	Magnitude of uncertainty
Temperature at BSR depth calibrated by heat flow studies	5–10 per cent
Temperature at BSR depth derived from accepted models for gas hydrate stability	10–20 per cent
Variable bottom water temperature	1–10 per cent
Conversion of seismic traveltimes to depth	1–5 per cent
⇒ Geothermal gradient	5–35 per cent
Conductivity from heat probes or gravity cores	~5 per cent
Conductivity from local relationships between seismic velocity/porosity/thermal conductivity	~5 per cent
Conductivity from global relationships between seismic velocity/porosity/thermal conductivity	5–30 per cent
Effect of gas hydrates on thermal conductivity structure	<5 per cent
⇒ thermal conductivity	5–30 per cent
⇒ heat flow	10–>50 per cent

that we did not include any error arising from the conversion of seismic traveltimes to depth. Possible errors in depth might be in the range of 5–20 m, depending on the depth to the BSR and the velocity data available. This issue is discussed in the appropriate seismic literature in much more detail. However, it is important to note that the errors discussed here are not necessarily real, but represent the uncertainty of the estimates.

In a simple fictional case study we show how errors may affect the calculation of the BSR-derived heat flow. We assume that the BSR occurs at 0.4 s two-way traveltime under the seafloor. Unfortunately, we had only a single-channel seismic streamer and no information on the velocity–depth structure. Therefore, we used a seismic velocity of 1650 m s^{-1}: because the seismic velocity of water-saturated sediment close to the seafloor is generally dominated by the properties of water, a velocity some 100 m s^{-1} faster than that of water is a reasonable assumption. Temperature at the seafloor was measured at 2 °C at a depth of 1200 m. Consequently, the BSR is determined to be at 330 m below seafloor or 1530 m below sea level, yielding a temperature at BSR depth of 15.37 °C (seawater–methane system). Conductivity was derived from the relationship of Horai (1981): 1.0 W m^{-1} K^{-1}. The geothermal gradient and heat flow are 40.5 K km^{-1} and 40.5 mW m^{-2}, respectively. A few weeks after the survey, a seismic refraction experiment was carried out yielding a seismic velocity of 1600 m s^{-1} in the uppermost 500 m. The geothermal gradient recalculated with a depth to the BSR of 320 m and a temperature of 15.32 °C is 41.6 K km^{-1}. The heat flow is 41.6 mW m^{-2}, i.e. 3 per cent higher. Both experiments were part of a pre-site survey for the ODP. Drilling and subsequent downhole measurements with the DVTP tool provided a temperature at the BSR (320 mbsf) that is 1.5 K lower than expected from the seawater–methane model. The thermal conductivity of sediments was determined by needle probe measurements, giving 1.15 W m^{-1} K^{-1}. Thus, the geothermal gradient and heat flow are 36.9 K km^{-1} and 42.5 mW m^{-2}, respectively. Most importantly, although the thermal gradient is 4.7 K km^{-1} (12 per cent) lower, the heat flow is reasonably similar because the gradient decrease was compensated for by the thermal conductivity, which increased by 0.15 W m^{-1} K^{-1} (15 per cent). If, however, thermal conductivity had decreased by 0.15 W m^{-1} K^{-1} instead, heat flow would have decreased by 25 per cent to 31.4 mW m^{-2}.

Application of constraints

On the Makran continental margin, Kaul *et al.* (2000) compared measured and BSR-derived heat flows. In terms of their results, the temperature at BSR depth must be 5–6 K lower than predicted by a seawater–methane system. Compared to the results from drilling (Fig. 2 and Table 1), this discrepancy seems to be unreasonably high. We therefore try to assess the Makran heat flow values using the constraints found in our study.

Kaul *et al.* (2000) used global relationships between seismic velocity and porosity. They applied both the Davis & Villinger (1992) and the Erickson & Jarrard (1998) relationships. As shown above, errors of 10–20 per cent may arise. To calculate conductivity from porosity, eq. (3) was used. In contrast to the best-fitting geometric mean of 2.5 W m^{-1} K^{-1} for the matrix conductivity found in this study (Fig. 5), they used a value of 3.9 W m^{-1} K^{-1}. This comparatively high value was chosen to account for the high *in situ* conductivity of 1.27 W m^{-1} K^{-1} found in the uppermost sediments. This value, however, is similar to measurements on the Chile Margin, where about 50 per cent of the values from seafloor samples gave a conductivity of about 1.25 W m^{-1} K^{-1} (Cande *et al.* 1987), which equals the average value of 1.25 W m^{-1} K^{-1} found in the drill sites (Fig. 6). The drill sites off Chile, like most other sites, show that there is no need to assume a strong depth dependence of thermal conductivity (Table 2). The uncertainties arising from both global velocity–porosity relationships and the high matrix conductivity may account for the BSR-derived heat flow values that are 40–50 per cent too high.

In our approach we use a very simple model, that is, a constant conductivity of 1.27 W m^{-1} K^{-1}, a seawater–methane system for gas hydrate stability and temperature measurements obtained in the water column. The depth to the BSR was derived from a joint seismic reflection and large-aperture experiment (Grevemeyer *et al.* 2000). A comparison of the geothermal gradient and heat flow derived from measurements with a Lister probe (Kaul *et al.* 2000) and BSR-derived values is presented in Fig. 9. Ignoring the highest and lowest values from heat probe measurements (which may indicate advection of heat), both techniques support the same heat flow within error bounds. Therefore, the seawater–methane system could be used to describe the stability of natural gas hydrates off Pakistan.

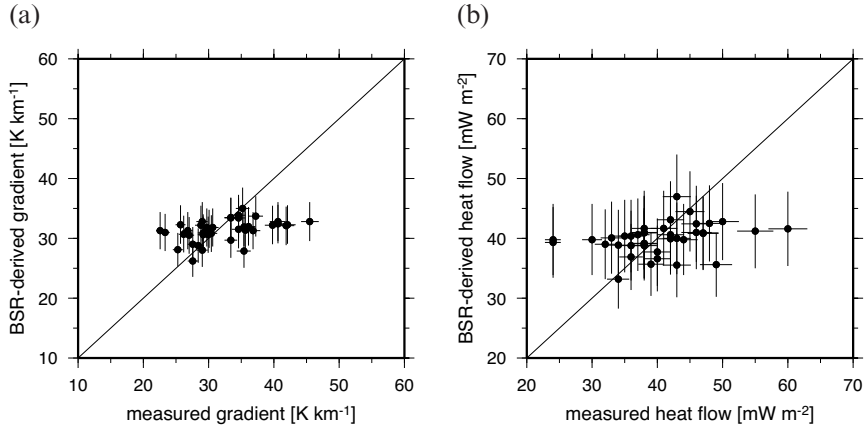

Figure 9. BSR-derived geothermal gradients and heat flow for the Makran Margin compared to determinations based on measurements with a Lister heat probe (Kaul *et al.* 2000).

Previous claims that the temperature might be 5–6 K lower may have resulted from inappropriate parameters used to calculate the thermal conductivity and hence the heat flow.

CONCLUSIONS

Results from five ODP legs drilled into both active and passive continental margins have been used to show and discuss errors and uncertainties arising from the estimation of heat flow from seismic BSRs. The constraints have been applied to a BSR off Pakistan and have been compared to heat flow values derived from heat probe measurements. A number of conclusions can be drawn.

(1) Downhole temperature measurements suggest that a seawater–methane system is appropriate for the calculation of temperatures at BSR depth. Nevertheless, capillary forces acting in fine-grained sediments, chemical impurities and non-equilibrium conditions may change the temperature by up to 4 K or even more. Therefore, thermal gradients could be incorrect by 10–20 per cent. In addition, variable bottom water temperatures may increase the uncertainty to $\sim$30 per cent.

(2) Calculation of downhole-log-derived *in situ* thermal conductivities indicate that typical concentrations of low-conductivity gas hydrate ($\sim$5–15 per cent saturation) do not have a considerable impact on the bulk thermal conductivity of sediments.

(3) Although thermal conductivity is strongly dependent on the porosity of sediment, decreasing porosity with depth did not affect the bulk conductivity between the BSR and the seabed significantly. A mean value provides roughly the same fit to the conductivity data from needle probe measurements on ODP drill cores as a porosity-dependent model.

(4) Estimates of the thermal conductivity based on global empirical relationships between seismic velocity, porosity and conductivity are often spurious. Errors of 20–30 per cent (or more) may arise. An assessment of the conductivity based on measurements taken in the seabed or in material recovered from the seafloor gives an even better fit.

(5) Application of the constraints to the Makran margin suggests that BSR-derived heat flow can be calculated using a very simple approach: using a mean value for the thermal conductivity derived from seafloor measurements and the thermal gradient calculated from the temperature at the seafloor and an accepted model for gas hydrate stability assuming a seawater–methane system.

We conclude that BSR studies can indeed be used to place additional constraints on the thermal state of continental margins. However, in addition to high-quality seismic data, a prerequisite is a large data set of thermal conductivities and oceanographic constraints. If the temperature at the BSR can be constrained by heat probe measurements, the resulting uncertainty/error of the assessment will be within 5–10 per cent of the estimated heat flow. If this additional information is not available, errors can reach 50–60 per cent of the calculated heat flow value.

ACKNOWLEDGMENTS

We are grateful to the Deutsche Forschungsgemeinschaft for supporting the Deep Sea Drilling Project and the Ocean Drilling Program for more than 20 years. Without all the scientists serving on drilling vessel *Joides Resolution*, this study would not have been possible. The logging data used in this study are from the ODP Online Logging Database at the Lamont Doherty Earth Observatory; Paul Wallace provided the thermal conductivity data from ODP Leg 164. We would like to thank Ben Clennell and Ingo Pecher, whose comments improved the manuscript. The Makran heat flow data were acquired under a grant from the Bundesminister für Bildung, Wissenschaft, Forschung und Technologie (03G0124A).

REFERENCES

Archie, G.E., 1942. The electrical resistivity log as an aid in determining some reservoir characteristics, *J. Petrol. Technol.,* **5,** 1–8.

Athy, L.F., 1930. Density, porosity and compaction of marine sedimentary rocks, *Am. Assoc. Petrol. Geol. Bull.,* **14,** 1–35.

Bangs, N.L., Sawyer, D.S. & Golovchenko, X., 1993. Free gas at the base of the gas hydrate zone in the vicinity of the Chile triple junction. *Geology,* **21,** 905–908.

Behrmann, J.H. *et al.*, 1992. *Proc. ODP Init. Repts,* **141**.

Brigaud, F. & Vasseur, G., 1989. Mineralogy, porosity and fluid control on thermal conductivity of sedimentary rocks, *Geophys. J. Int.,* **98,** 525–542.

Brown, K.M. & Bangs, N.L., 1995. Thermal regime of the Chile triple junction: constraints provided by downhole temperature measurements and distribution of gas hydrate, *Proc. ODP Init. Repts,* **141,** 259–275.

Cande, S.C., Leslie, R.B., Parra, J.C. & Hobart, M., 1987. Interaction between the Chile Ridge and Chile trench: geophysical and geothermal evidence, *J. geophys. Res.,* **92,** 495–520.

Claypool, G.W. & Kaplan, I.R., 1974. The origin and distribution of methane in marine sediments, in *Natural Gases in Marine Sediments*, pp. 99–139, ed. Kaplan, I.R., Plenum, New York.

Clennell, M.B., Hovland, M., Booth, J.S., Henry, P. & Winters, W.J., 1999. Formation of natural gas hydrates in marine sediments; 1 conceptual model of gas hydrate growth conditioned by host sediment properties, *J. geophys. Res.,* **104,** 22 985–23 003.

Collett, T.S. & Ladd, J., 2000. Detection of gas hydrate with downhole logs and assessment of gas hydrate concentrations (saturations) and gas volumes on the Blake Ridge with electrical resistivity log data, *Proc. ODP Sci. Results,* **164,** 179–191.

Davis, E.E. & Villinger, H., 1992. Tectonic and thermal structure of the middle valley sedimented rift, northern Juan de Fuca Ridge, *Proc. ODP Init. Repts,* **139,** 9–41.

Davis, E.E., Hyndman, R.D. & Villinger, H., 1990. Rates of fluid expulsion across the northern Cascadia accretionary prism: constraints from new heat flow and multichannel seismic reflection data, *J. geophys. Res.,* **95,** 8869–8889.

Davis, E.E., Becker, K., Wang, K. & Carson, B., 1995. Long-term observations of pressure and temperature in hole 892B, Cascadia accretionary prism, *Proc. ODP Sci. Results,* **146,** 299–311.

Davis, E.E., Villinger, H., MacDonald, R.D., Meldrum, R.D. & Grigel, J., 1997. A robust rapid-response probe for measuring bottom-hole temperatures in deep-ocean boreholes, *Mar. geophys. Res.,* **19,** 267–281.

Davis, E.E. *et al.*, 1999. Regional heat flow variations across the sedimented Juan de Fuca Ridge eastern flank: constraints on lithospheric cooling and lateral hydrothermal heat transport, *J. geophys. Res.,* **104,** 17 675–17 689.

Dickens, G.R. & Quinby-Hunt, M.S., 1994. Methane hydrate stability in seawater, *Geophys. Res. Lett.,* **21,** 2115–2118.

Dickens, G.R., Paull, C.K., Wallace, P. & the ODP Leg 164 Scientific Party, 1997. Direct measurements of in situ methane quantities in a large gas-hydrate reservoir, *Nature,* **385,** 426–428.

Englezos, P. & Bishnoi, P.R., 1988. Prediction of gas hydrate formation conditions in aqueous electrolyte solution, *Am. Inst. Chem. Eng. J.,* **34,** 1718–1721.

Erickson, S.E. & Jarrard, R.D., 1998. Velocity-porosity relationships for water-saturated siliclastic sediments, *J. geophys. Res.,* **103,** 30 385–30 406.

Fisher, A.T. & Becker, K., 1993. A guide to ODP tools for downhole measurements, *ODP Tech. Note,* **10**.

Fisher, A.T. & Hounslow, M.W., 1990. Transient fluid flow through the toe of the Barbados accretionary complex: constraints from ODP leg 110 heat flow studies and simple models, *J. geophys. Res.,* **95,** 8845–8858.

Grevemeyer, I., Rosenberger, A. & Villinger, H., 2000. Natural gas hydrates on the continental slope off Pakistan: constraints from seismic techniques, *Geophys. J. Int.,* **140,** 295–310.

Guerin, G., Goldberg, D. & Meltser, A., 1999. Characterization of in situ elastic properties of gas hydrate bearing sediments on the Blake Ridge, *J. geophys. Res.,* **104,** 17 781–17 795.

Hamilton, E.L., 1971. Elastic properties of marine sediments, *J. geophys. Res.,* **78,** 579–604.

Handa, Y.P. & Stupin, D., 1992. Thermodynamic properties and dissociation characteristics of methane and propane hydrates in 70-Å-radius silica gel pores, *J. Phys. Chem.,* **96,** 8599–8603.

Henry, P., Thomas, M. & Clennell, M.B., 1999. Formation of natural gas hydrates in marine sediments; 2 thermodynamic calculations of stability conditions in porous sediments, *J. geophys. Res.,* **104,** 23 005–23 022.

Horai, K., 1981. Thermal conductivity of sediments and igneous rocks recovered during Deep Sea Drilling Project leg 60, *DSDP Init. Repts,* **60,** 807–834.

Horai, K. & von Herzen, R., 1986. Measurements of heat flow on leg 86 of the Deep Sea Drilling Project, *DSDP Init. Repts,* **86,** 759–777.

Hovland, M., Gallagher, J.W., Clennell, M.B. & Lekvam, K., 1997. Gas hydrate and free gas volumes in marine sediments: example from the Niger delta front, *Mar. Petrol. Geol.,* **14,** 245–355.

Hyndman, R.D. & Wang, K., 1993. Thermal constraints on the zone of major thrust earthquake failure: the Cascadia subduction zone, *J. geophys. Res.,* **98,** 2039–2060.

Hyndman, R.D. & Wang, K., 1995. The rupture zone of Cascadia great earthquakes from current deformation and the thermal regime, *J. geophys. Res.,* **100,** 22 133–22 154.

Hyndman, R.D., Davis, E.E. & Wright, J.A., 1979. The measurement of marine geothermal heat flow by a multi-penetration probe with digital acoustic telemetry and in situ thermal conductivity, *Mar. geophys. Res.,* **4,** 181–205.

Hyndman, R.D., Langseth, M.G. & von Herzen, R.P., 1987. Deep Sea Drilling Project geothermal measurements: a review, *Rev. Geophys.,* **25,** 1563–1582.

Hyndman, R.D., Foucher, J.P., Yamano, M., Fisher, A.T. & the ODP Leg 131 Scientific Party, 1992. Deep sea bottom simulating reflectors: calibration of the base of the hydrate stability field as used for heat flow estimates, *Earth planet. Sci. Lett.,* **109,** 289–301.

Kaul, N., Rosenberger, A. & Villinger, H., 2000. Comparison of measured and BSR-derived heat flow values, Makran accretionary prism, Pakistan, *Mar. Geol.,* **164,** 37–51.

Kvenvolden, K.A., 1993. Gas hydrates—geological perspective and global change, *Rev. Geophys.,* **31,** 173–187.

Lister, C.R.B., 1979. The pulse probe method of conductivity measurements, *Geophys. J. R. astr. Soc.,* **57,** 451–461.

MacKay, M.E., Jarrard, R.D., Westbrook, G.K., Hyndman, R.D. & the ODP Leg 146 Scientific Party, 1994. Origin of bottom simulating reflectors: geophysical evidence from the Cascadia accretionary prism, *Geology,* **22,** 459–462.

Matsumoto, R. & Borowski, W.S., 2000. Gas hydrate estimates from newly determined oxygen isotropic fraction and $\delta^{18}O$ anomalies of the interstitial waters: leg 164, Blake Ridge, *Proc. ODP Sci. Results,* **164,** 59–65.

Minshull, T.A. & White, R.S., 1989. Sediment compaction and fluid migration in the Makran accretionary prism, *J. geophys. Res.,* **94,** 7387–7402.

Oleskevich, D.A., Hyndman, R.D. & Wang, K., 1999. The updip and downdip limits to great subduction earthquakes: thermal and structural models of Cascadia, south Alaska, SW Japan, and Chile, *J. geophys. Res.,* **104,** 14 965–14 991.

Paull, C.K. *et al.*, 1996. *Proc. ODP Init. Repts,* **164**.

Pecher, I.A., 1995. Seismic studies of bottom simulating reflectors at the convergent margins offshore Peru and Costa Rica, *PhD thesis,* GEOMAR, Rept, 47, Kiel, Germany.

Pelayo, A. & Wiens, D., 1992. Tsunami earthquakes: slow thrust-faulting events in the accretionary wedge, *J. geophys. Res.,* **97,** 15 321–15 337.

Pribnow, D., Davis, E.E. & Fisher, A.T., 2000. Borehole heat flow along the eastern flank of the Juan de Fuca Ridge including effects of anisotropy and temperature dependence of sediment thermal conductivity, *J. geophys. Res.,* **105,** 13 449–13 456.

Radcliffe, E.H., 1960. The thermal conductivities of ocean sediments, *J. geophys. Res.,* **65,** 1563–1541.

Ruppel, C., 1997. Anomalously cold temperatures observed at the base of gas hydrate stability zone on the US passive continental margin. *Geology,* **25,** 699–704.

Ruppel, C., von Herzen, R.P. & Bonneville, A., 1995. Heat flux through an old (~175 Ma) passive margin: offshore southeast United States, *J. geophys. Res.,* **100,** 20 037–20 057.

Shipley, T.H., Houston, M.H., Buffler, R.T., Shaub, F.J., McMillen, K.J., Ladd, J.W. & Worzel, J.L., 1979. Seismic reflection evidence for the widespread occurrence of possible gas-hydrate horizons on continental slope and rises, *Am. Assoc. Petrol. Geol. Bull.,* **63,** 2204–2213.

Sloan, D.E., 1990. *Clathrate Hydrates of Natural Gases,* Marcel Dekker, New York.

Spangenberg, E., 2000. Modeling of the influence of gas hydrate content on the electrical properties of porous sediments, *J. geophys. Res.,* in press.

Stoll, R.D. & Bryan, G.M., 1979. Physical properties of sediments containing gas hydrates, *J. geophys. Res.,* **84,** 1629–1634.

Suess, E. *et al.*, 1988. *Proc. ODP Init. Repts,* **112**.

Taira, A. *et al.*, 1991. *Proc. ODP Init. Repts,* **131**.

Tohidi, B., Danesh, A. & Todd, A.C., 1995. Modeling single and mixed electrolyte solutions and its applications to gas hydrates, *Chem. Eng. Res. Des.,* **73,** 464–472.

Tryon, M.D., Brown, K.M., Torres, M.E., Tréhu, A.M., McManus, J. & Collier, R.W., 1999. Measurements of transience and downward fluid flow near episodic methane gas vents, Hydrate Ridge, Cascadia, *Geology,* **27,** 1075–1078.

Tucholke, B.E., Bryan, G.M. & Ewing, J.I., 1977. Gas-hydrate horizons detected in seismic profile data from the western North Atlantic, *Am. Assoc. Petrol. Geol. Bull.,* **61,** 698–707.

Villinger, H. & Davis, E.E., 1987. A new reduction algorithm for marine heat flow measurements, *J. geophys. Res.,* **92,** 12 846–12 856.

Villinger, H., Langseth, M.G., Gröschel-Becker, H.M. & Fisher, A.T., 1994. Estimating in-situ thermal conductivity from log data, *Proc. ODP Init. Repts,* **139,** 545–552.

von Herzen, R. & Maxwell, M.E., 1959. The measurement of thermal conductivity of deep sea sediments by a needle probe method, *J. geophys. Res.,* **64,** 1557–1563.

Westbrook, G.K. *et al.*, 1994. *Proc. ODP Init. Repts,* **146**.

Wood, W.T. & Ruppel, C., 2000. Seismic and thermal investigations of the Blake Ridge gas hydrate area: a synthesis, *Proc. ODP Sci. Results,* **164,** 253–264.

Yamano, M. & Uyeda, S., 1990. Heat flow studies in the Peru trench subduction zone, *Proc. ODP Sci. Results,* **112,** 653–661.

Yamano, M., Uyeda, S., Aoki, Y. & Shipley, T.H., 1982. Estimates of heat flow derived from gas hydrates, *Geology,* **10,** 339–343.

Zakrzewski, M. & Handa, Y.P., 1993. Thermodynamic properties of ice and of tetrahydrofuran hydrate in confined geometries, *J. Chem. Thermodyn.,* **25,** 631–637.

Zwart, G., Moore, J.C. & Cochrane, G.R., 1996. Variations in temperature gradients identify active faults in the Oregon accretionary prism, *Earth. planet. Sci. Lett.,* **139,** 485–495.